

NON-PROTECTIVE OXIDE FORMATION IN HIGH ENTROPY CARBIDE ULTRA-HIGH TEMPERATURE CERAMICS

Lavina Backman, Elizabeth J. Opila

Department of Materials Science and Engineering, University of Virginia, Charlottesville, VA 22904

Abstract:

Bulk samples of high entropy ultra-high temperature ceramics (UHTCs) of composition (HfNbTaTiZr)C was fabricated via high energy ball milling and spark plasma sintering. ZrC bulk samples were also prepared via spark plasma sintering. Oxidation behavior of both carbide compositions was tested at 1500°C, 1700°C and 1800°C using a resistive heating apparatus in one atmosphere reduced PO₂ oxygen/argon gas mixtures for times up to 15 minutes. Oxidation kinetics were determined from the variation of material consumption vs. time. The oxide scale was characterized using SEM and EDS. The high entropy carbide exhibited grain boundary oxidation, non-protective oxide formation and higher material consumption rates in almost all cases, when compared to ZrC.

Introduction

A new paradigm has emerged in the design of new materials that is currently being applied to metals and ceramics¹⁻³, wherein configurational entropy is leveraged to stabilize solid solutions. This entropy stabilization allows for new compositions to be designed and explored. Applying this approach to ultra-high temperature ceramics has been the focus of significant research interest.

Ultra-high temperature ceramics are being considered for use in extreme environment applications, where thermochemical stability above 1700°C is an important consideration. Among these materials, Hf and Zr carbides and borides are among the chief candidates, and their oxidation behavior is well characterized (references). However, UHTCs are generally limited by their rapid reaction rates with oxygen⁴. In particular, ZrC and HfC have been reported to oxidize non-protectively below 1800°C⁵.

Berkowitz-Mattuck et al.⁶ expected that the rate of ZrC oxidation at low partial pressures and high temperatures is reaction controlled; they were able to observe this, but largely saw gas phase diffusion due to their experimental set-up. They found that these carbides oxidized preferentially along the grain boundaries. Gozzi et al. also found that the oxidation of ZrC largely followed linear kinetics and only approached parabolic kinetics at low

temperatures and higher partial pressures of oxygen (pO₂). Gasparrini et al. also found linear oxidation kinetics for ZrC, and observed the oxidation mechanism to be oxygen diffusion through an oxide scale containing amorphous carbon into the carbide^{7,8}.

Elucidating the oxidation mechanisms and building a framework to understand the oxidation behavior of high entropy carbides requires an understanding of the mechanisms and how they vary from that of monocarbides such as HfC and ZrC. To that end, experiments were conducted to measure material degradation as a function of pressure, temperature and time. These dependencies were compared to the oxidation behavior of ZrC and ZrB₂. Zirconium is a constituent of the candidate composition tested, and forms the basis of widely studied UHTC materials, as discussed previously.

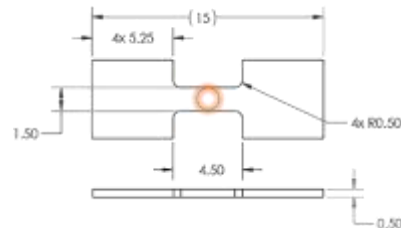


Figure 1: Dogbone specimen configuration. Approximate hot zone (diameter 1.5 mm) shown in orange.

Experimental Procedure

Materials chosen for preliminary study are carbides and borides containing Group IV and Group V elements: Hf, Zr, Ti, Ta and Nb. Ta has been an extensively studied elemental addition for high temperature UHTCs^{9,10}, and in the context of this work, have the ability to form solid solutions with Hf and Zr based compounds. Next to Ti based oxides, its oxides have the highest melting temperature among the species under consideration. This composition is also one of the first compositions for which single phase, solid solutions could be made.

The (HfZrTiTaNb)C specimen tested in this work was prepared by high energy ball milling and spark plasma sintering commercially available powders (Alfa Aesar Haverhill, MA) at the University of California – San Diego (UCSD, La Jolla, CA). The sintered samples were machined at Bomas Machine Specialties (Somerville, MA) into thin dogbone specimens shown in **Figure 1**.

These dogbones were then loaded into a resistive heating system, schematic shown in **Figure 2**. The samples were heated to the required temperature through Joule heating, and the temperature was controlled by a proportional-integral-derivative (PID) controller and an emissivity correcting one-color pyrometer (Pyrofiber Lab PFL-0865-0790-2500C311, Pyrometer Instrument Company, Ewing Township, NJ).

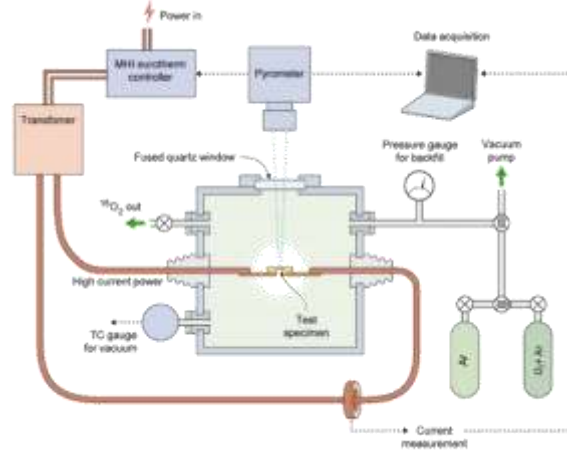


Figure 2: Schematic of the resistive heating experimental set-up. Specimen shown is of different configuration for clarity.

The controlled region, or hot zone, is shown with respect to the dogbone specimen in **Figure 1**. The samples were ramped to temperature in ultra-high purity argon (Praxair, Danbury, CT), and the oxidizing gas turned on at temperature. The samples were oxidized at 0.1%, 0.5% and 1% O₂ for 2-15 mins. Low partial pressures of oxygen were chosen as these more closely reflect the environment during re-entry at hypersonic speeds. The low partial pressures of oxygen used also result in lower oxidation rates allowing for longer exposures. After oxidation, the samples were manually fractured across the hot zone, and the

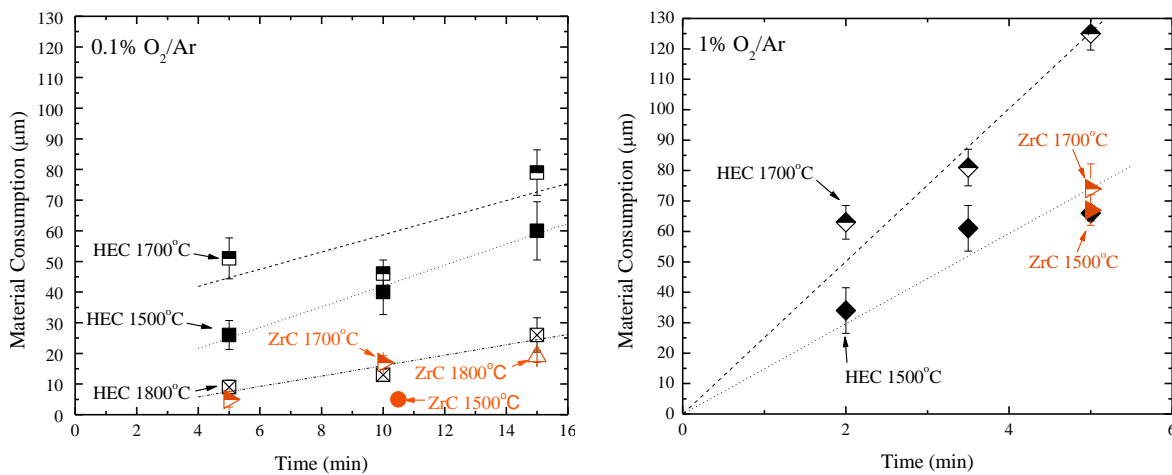


Figure 3: (HfZrTiTaNb)C and ZrC oxidized at various temperatures in (left) 0.1% O₂ and (right) 1% O₂. ZrC data points are shown in orange.

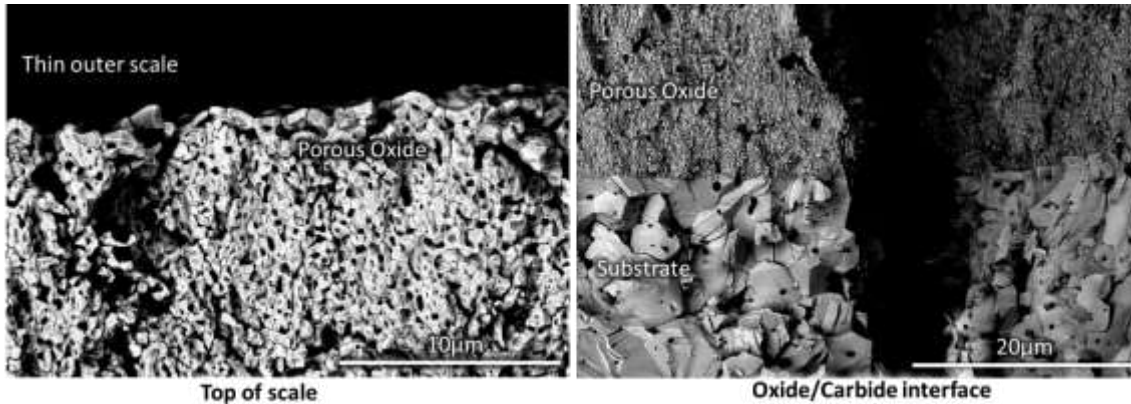


Figure 5: Back-scattered electron image of the (left) top of the cross-section of the oxide scale formed on ZrC exposed to 1%O₂ at 1700°C for 5 minutes and (right) of the same oxide scale at the oxide-carbide interface, also in cross-section.

cross-sections were examined in a scanning electron microscope (SEM, FEI Quanta 650, FEI-Thermo Fisher Scientific, Hillsboro, Oregon). The oxide morphology in both plan view and cross section were characterized using SEM and energy dispersive spectroscopy (EDS, EDS, Oxford Instruments Aztec X-Max^{AN} 150, Concord, MA). The oxide products were also characterized using X-ray diffraction (XRD, PANalytical X'Pert Pro MPD or PANalytical Empyrean, Almelo, The Netherlands).

Results

A limited number of samples of ZrC were available, thus only selected conditions were tested to gauge the difference between its material consumption and that of (HfZrTiTaNb)C. The bounding partial pressures of oxygen tested, 0.1% and 1% O₂ are shown in **Figure 3**. (HfZrTiTaNb)C exhibits higher material consumption compared to ZrC at 1500°C and 1700°C, with the highest consumption occurring at 1700°C in 0.1% O₂. The high entropy carbide not only exhibits lower material consumption at 1800°C compared to other temperatures, but also shows comparable material consumption to ZrC tested under the same conditions. At 1% O₂, the high entropy carbide exhibits similar material consumption to ZrC, but the ZrC performs better at 1700°C.

The material consumption's dependence on pO₂ was compared for the high entropy carbide and ZrC. If similar mechanisms controlled the oxidation rate in both materials, then the partial pressure dependence would be similar. However, a much shallower pO₂ dependence is seen for the high entropy carbide, compared to ZrC tested here. The micrograph shown in Figure 4 indicates extensive oxidation along what appear to be the grain boundaries.

Figure 5 shows the top of the scale formed on ZrC, and the interface between the oxide and the carbide. There was no evidence of oxidation along the grain boundaries – instead, a sharp interface is seen.

Discussion

Material consumption on high entropy carbides are generally higher than zirconium carbide in 0.1% O₂. The exception here is 1800°C, which is also the condition wherein material consumption counterintuitively drops to below that at 1500°C and 1700°C, suggesting a change in mechanism in the oxidation of high entropy carbides around that temperature. Characterization completed thus far show a reduction in the depth to which oxidation along grain boundaries can be detected. Further experiments and characterization are needed to elucidate this change, but one hypothesis is that a less porous oxide, or an oxide with a different

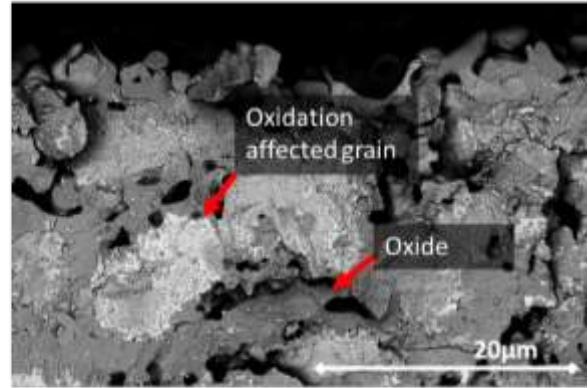
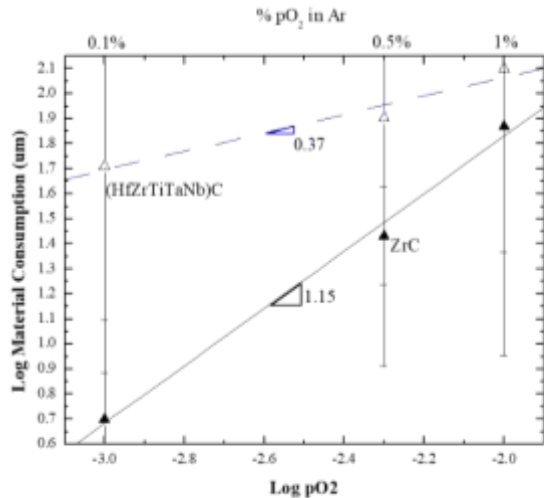


Figure 4: (Left) Log-log plot of the material consumption versus partial pressure of oxygen at 1700°C and 5 minutes. Shown in triangles and blue dotted line are the data points corresponding to the high entropy carbide, while those for the ZrC are shown in black. (Right) A back-scattered image of the top of the resulting oxidized region in (HfZrTiTaNb)C shown in cross section after exposure in 1%O₂ at 1700°C for 5 minutes.

composition forms, which mitigates oxidation along the grain boundaries. Similarly, minimal oxidation along grain boundaries is observed in the 1500°C, 1%O₂ case. Thus, the poorer performance at all other conditions is attributed to grain boundary oxidation and preferential oxidation. Apparent linear kinetics in the high entropy carbides, along with evidence of pO₂ dependence and generally non-protective oxides at most conditions tested suggest oxidation rates in those cases are reaction controlled.

Conclusions

High entropy carbides generally exhibit non-protective oxide formation, with some exceptions. This non-protective oxide formation translated to poorer oxidation resistance compared to ZrC. Linear kinetics, pO₂ dependence, and non-protective oxide formation suggest that oxidation of high entropy carbides is reaction limited. In the cases where oxidation behavior was similar to ZrC, minimal grain boundary oxidation was noted, suggesting a more protective oxide formed in those conditions.

Acknowledgements

This work is supported by the U.S. Office of Naval Research MURI program (grant no. N00014-15-1-2863) and the Virginia Space Grant Fellowship. The authors would also like to thank the Vecchio group at the University of California San Diego for providing the materials for this study.

References

1. Harrington, T. J. *et al.* Phase stability and mechanical properties of novel high entropy transition metal carbides. *Acta Materialia* **166**, 271–280 (2019).
2. Gild, J. *et al.* High-Entropy Metal Diborides: A New Class of High-Entropy Materials and a New Type of Ultrahigh Temperature Ceramics. *Sci Rep* **6**, (2016).
3. Miracle, D. B. High entropy alloys as a bold step forward in alloy development. *Nature Communications* **10**, 1805 (2019).
4. Wuchina, E., Opila, E., Opeka, M., Fahrenholtz, W. & Talmy, I. UHTCs: ultra-high temperature ceramic materials for extreme environment applications. *The Electrochemical Society Interface* **16**, 30 (2007).

5. Opeka, M. M., Talmy, I. G. & Zaykoski, J. A. Oxidation-based materials selection for 2000°C + hypersonic aerosurfaces: Theoretical considerations and historical experience. *Journal of Materials Science* **39**, 5887–5904 (2004).
6. Berkowitz-Mattuck, J. B. High-Temperature Oxidation: IV . Zirconium and Hafnium Carbides. *Journal of The Electrochemical Society* **114**, 1030–1033 (1967).
7. Gasparrini, C., Chater, R. J., Horlait, D., Vandeperre, L. & Lee, W. E. Zirconium carbide oxidation: Kinetics and oxygen diffusion through the intermediate layer. *Journal of the American Ceramic Society* **101**, 2638–2652 (2018).
8. Gasparrini, C. Oxidation of zirconium and uranium carbides. (2018).
9. Opila, E., Levine, S. & Lorincz, J. Oxidation of ZrB₂- and HfB₂-based ultra-high temperature ceramics: Effect of Ta additions. *Journal of Materials Science* **39**, 5969–5977 (2004).
10. Silvestroni, L., Sciti, D., Balat-Pichelin, M. & Charpentier, L. Zirconium carbide doped with tantalum silicide: Microstructure, mechanical properties and high temperature oxidation. *Materials Chemistry and Physics* **143**, 407–415 (2013).